DOI: 10.24352/UB.OVGU-2017-089 TECHNISCHE MECHANIK, 37, 2-5, (2017), 120 – 128
submitted: June 19, 2017

Strength Assessment of a Precession Driven Dynamo

S. Rother, M. Beitelschmidt

A pressure vessel, which shall be filled with eight tons of liquid sodium, has to be designed for a large-scale experimental setup to investigate flow-induced magnetic fields. In addition to the centrifugal forces and gyroscopic loads induced by the rotation about two non-parallel axes, the complex internal pressure distribution, the imbalance of the container, as well as the thermal loads resulting from the elevated temperatures, which are required for the experiments, must be taken into account. This leads to several millions of load cases. That is why a calculation procedure is developed using the finite element method, which strongly reduces the computational complexity by utilizing sector symmetry, load case decomposition and superposition. Here, the focus is to determine the most critical load cases, which will be used for the strength assessment, regarding both the static and the fatigue strength. Besides the structural strength, the welded joints and the bolted joints are analyzed. Therefore, nonlinear effects are considered, for example the contact status of the bolted joints. The submodelling technique is used to investigate structural details.

1 Introduction

Within the framework of the project DRESDYN (DREsden Sodium facility for DYNamo and thermohydraulic studies) at the Helmholtz-Zentrum Dresden-Rossendorf (HZDR) experimental investigations of flow-induced magnetic fields will be performed (Stefani et al., 2012). This is comparable to the processes in the outer earth's core, in which iron and nickel are present in liquid form. In conjunction with an existing magnetic field, the flows of the liquid metal induce an electric current, which in turn produces a magnetic field. If the flows show a sufficiently helical shape, the original field is amplified and a stable magnetic field develops, called the homogeneous dynamo effect. The aim of the experiment is to investigate whether rotation and precession of astronomical objects serve as source for the described self-excitation of magnetic fields. The rotation and precession corresponds to the rotation of the earth about its axis within 24 h and the rotation of the earth's axis around the normal of the ecliptic plane with a cycle of 25,700 years.

According to Stefani et al. (2008) the formation of the described flow phenomena requires a critical magnetic Reynolds number $R_m = \mu_0 \sigma v L$, where μ_0 describes the magnetic field constant, σ the electrical conductivity, v the flow velocity, and L a characteristic length. Since the dimensions that can be realized in the test facility are limited, high rotational speeds are necessary. Sodium is chosen as liquid metal, which on the one hand is characterized by a low density, a low melting temperature and a high electrical conductivity, but on the other hand ignites when exposed to air humidity and thus requires strict safety precautions. To avoid corrosion, all components being in contact with sodium will be made of austenitic steel 1.4571.

The test facility designed by SBS Bühnentechnik GmbH is shown in Figure 1. A cylindrical pressure vessel with an inner diameter and a length of two meters, which has conical ends and can be filled with about eight tons of liquid sodium, is located in its center. The vessel shall rotate with a maximum frequency of 10 Hz and is positioned on a platform, which itself can rotate with up to 1 Hz about the vertical axis. The angle between the two rotation axes can be varied between $45°$ and $90°$ by a swivel frame.

The required flows should develop inside the cylindrical volume in the center of the pressure vessel (Figure 2). Rectangular wings can be extended into the flow to guide the fluid and thus reduce the turbulence. 40 sensor flanges in total are distributed on the cylinder wall allowing access for the measurement equipment. Because of the two rotations, no equalization of the volume expansion to the outside is possible. Therefore, the thermal expansion due to the warming of the sodium must be internally compensated. For this purpose, two argon-filled compensators in the cones prevent a critical rise of pressure. The conical shape is necessary to empty the container completely at a swivel angle of $42°$.

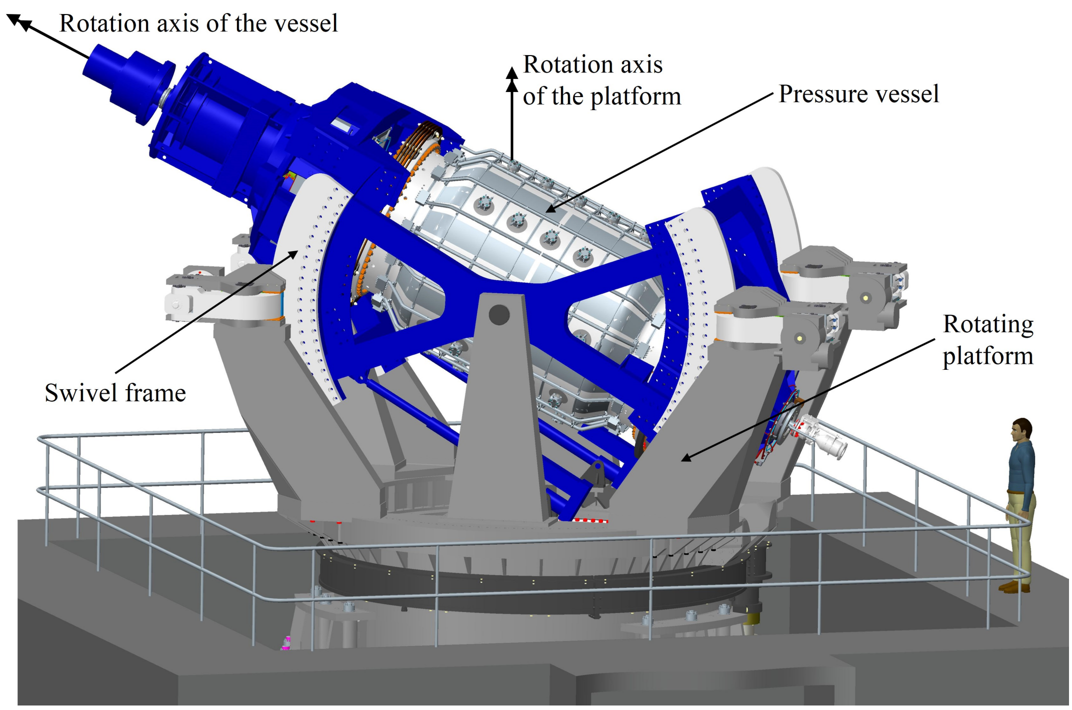

Figure 1: Setup of the test facility (provided by SBS Bühnentechnik GmbH).

As a result of the high rotational speeds and the hazard potential of the sodium, failure during operation must be reliably excluded. That is why the strength assessment of the vessel is performed in accordance with the FKM Guideline (FKM, 2012), using the finite element method (FEM) to determine the stresses. The FKM Guideline is also used to assess the welded joints, while the bolted joints are evaluated according to VDI 2230 Part 1 (2014). For the following experimental validation of the numerically calculated pressure distributions water is used instead of sodium.

2 Loads

Determining the stresses requires the consideration of all loads present at the structure, which are shown in Figure 3. The mechanical loads result from the rotation about two non-parallel axes, leading to a gyroscopic moment of almost $8 \cdot 10^6$ Nm. The rotation about the longitudinal axis of the container is described by the angular velocity ω_1 in the model, while the platform rotation is expressed by the angular velocity of the global reference system ω_2. The ratio of the angular velocities describes the precession ratio

$$\eta = \frac{\omega_2}{\omega_1}. \tag{1}$$

In addition, the radial and the axial imbalance have to be taken into account. Since the latter directly results from the asymmetric structure, especially at the bearings, it is explicitly included in the finite element model and thus does not require a separate consideration. In contrast, the radial imbalance due to manufacturing-related inaccuracies cannot be completely compensated during balancing. The defined balancing quality limits its maximum value, but its direction is unknown. As a consequence, the most unfavorable load combination has to be used for the strength assessment. The weight force is also considered, although it is of minor importance because of its small magnitude.

Much higher loads result from the fluid-structure interaction, whereby the pressure distribution strongly depends on the precession ratio (Figure 4). In case of no precession ($\eta = 0$), the pressure distribution is equal to that of a solid-body rotation. Hence, the pressure p increases with the radius r corresponding to $p \sim r^2$ and reaches a maximum of 20.7 bar. With rising precession ratio, the gyroscopic moment acting on the fluid leads to a pressure difference in the circumferential direction. Since the pressure distribution is constant in the coordinate system of the platform and does not rotate with the container, a cyclic load is caused. At high precession ratios ($\eta \to 0.1$), the former laminar flow turns into a turbulent flow, which accompanies with a significant decrease of the pressure

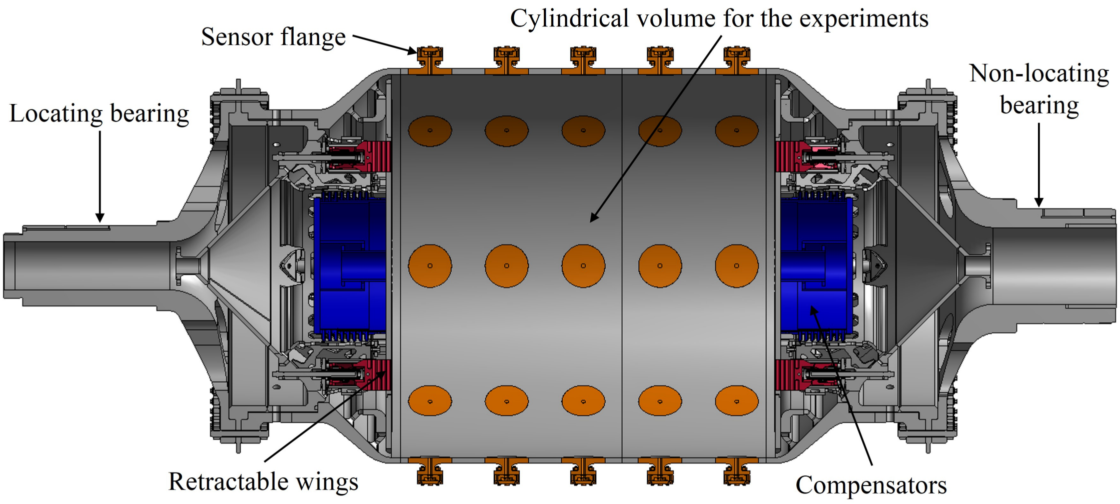

Figure 2: Sectional view of the pressure vessel.

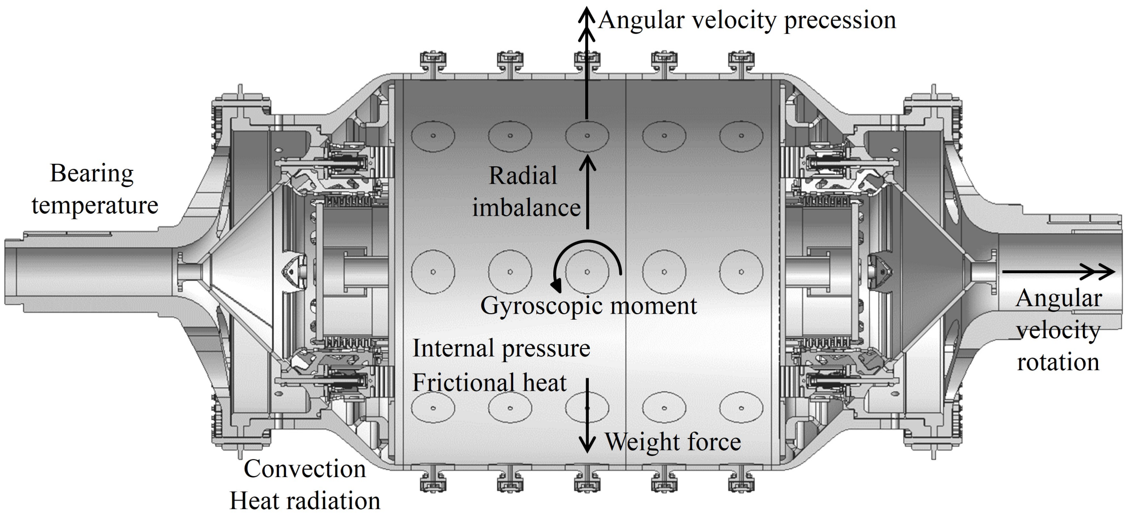

Figure 3: Overview of the loads present at the vessel for a swivel angle of 90°.

maximum. Because of the strong guidance of the fluid in the conical volumes of the vessel due to the numerous internal installations, the pressure distribution corresponds to a solid-body rotation for all precession ratios. This can lead to high pressure differences at the internal walls between the cylinder and the cones.

As the sodium experiments will be performed in a temperature range between 110 °C and 170 °C, thermal loads have to be taken into account to determine the thermal stresses. The ambient air is restricted to a maximum temperature of 60 °C in order to ensure the functionality of all electronic devices. The temperature difference between the surface and the environment causes a heat transfer by convection and heat radiation. Due to the high surface speed of the vessel ($\approx$ 65 m/s), forced convection is of particular importance even for the water experiment where the maximum temperature is limited to 85 °C. At high precession ratios, a large portion of the applied engine power of 800 kW is converted into heat by friction due to turbulence. So, the sodium warms up from 110 °C to 170 °C within about 25 minutes. In contrast, at low precession ratios corresponding to a laminar flow the sodium cools down from the selected initial temperature of 170 °C, since no appreciable heat conversion occurs. As a result of the low heat conductivity of the stainless steel, high temperature gradients are obtained in the vessel, which are determined in a transient analyses and are accompanied by high thermal stresses.

All described loads are superimposed for the strength assessment of the vessel. Due to the numerous influencing variables such as precession ratio, swivel angle, angle of rotation, direction of the radial imbalance and number of time steps for the computation of the thermal stresses, several millions of load cases occur. Thereby, the rotational

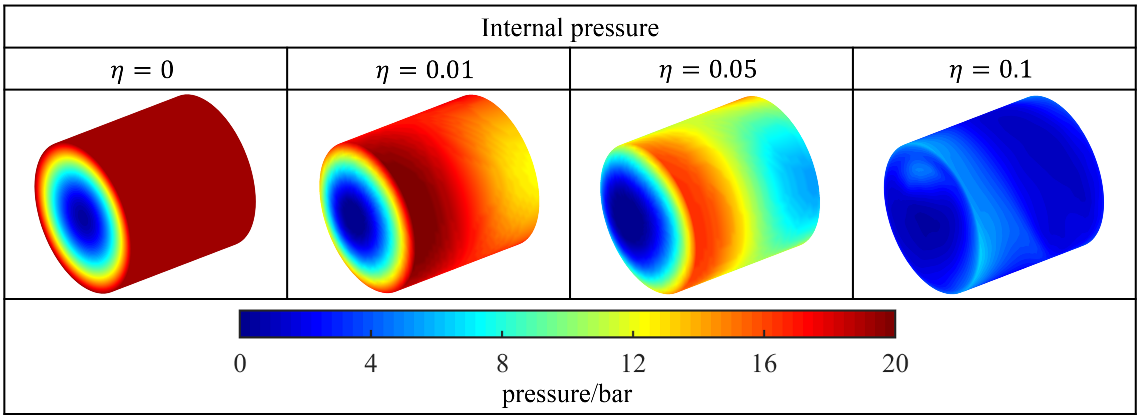

Figure 4: Pressure distribution on the cylinder wall as a function of the precession ratio (Giesecke et al., 2014; Stefani et al., 2014).

motion is discretized in steps of $5°$. Since a numerical solution of all load cases is not possible, the number of load steps has to be reduced by several orders of magnitude. For this purpose, a calculation algorithm has been developed which will be discussed in more detail in the next section.

3 Computation Algorithm

Figure 5 illustrates the general calculation process starting with the geometry, which is provided by the construction department, ending with the visualization of the utilization ratios. Here, the focus is on the computation of the stresses and the determination of the most critical load cases. Hence, the number of load cases solved within the finite element software has to be reduced from several millions to a manageable level. This requires a more precise analysis of the loads, the geometry and the material properties. The aim is to decompose the complex loads and afterwards to superpose the resulting stresses. The decoupling of the thermal and the mechanical field problem resulting from neglecting the piezocaloric effect, is an essential precondition. Therefore, the temperature field is computed in the first step before determining the thermal stresses. The temperature dependence of the material properties is negligible in the examined temperature intervals. In accordance with the FKM Guideline linear-elastic material behavior has been assumed (FKM, 2012). Furthermore, the bolted joints are linearized for the load case identification and the components are connected by bonded contact in the clamping area as described for model class I of VDI 2230 Part 2 (2014). Since a large sliding distance at the interface has to be avoided in general, this linearization does not constitute a restriction with respect to the global structural behavior. The resulting linear model is valid for the applied load case superposition. However, a separate analysis of the bolted joints has to be performed afterwards.

3.1 Computation of Stresses

Three different angles between the two angular velocity vectors are considered for the strength assessment. On the one hand, the horizontal position of the container (swivel angle $90°$) and on the other hand a swivel angle of $45°$, taking into account both directions of platform rotation. It is necessary to distinguish between these two variants of rotation directions, as for one case the effective angular velocity of the container increases while it decreases for the other one. This has a strong influence on the expected pressure distribution. Preliminary numerical studies proved that a restriction to four precession ratios ensures a safe dimensioning. In addition to the cases of no precession ($\eta = 0$) and maximum precession ($\eta = 0.1$), these precession ratios are $\eta = 0.03$, where the highest pressure amplitude occurs, and $\eta = 0.08$. This latter is a combination of a high pressure amplitude and a large gyroscopic moment, because it is present shortly before turning from the laminar to the turbulent flow.

As it can be seen in Figure 6, the stress computation is divided into three parts and is performed for each swivel angle and all four precession ratios. First, the thermal stresses are calculated, which is connected to the transient solution of the temperature field and takes place at intervals of 100 s. Because of the model symmetry and the symmetrical thermal load, the use of a quarter model is sufficient at this point. This is followed by the determination of the stresses due to the radial imbalance and the other mechanical loads. In the latter case, the rotation angle of

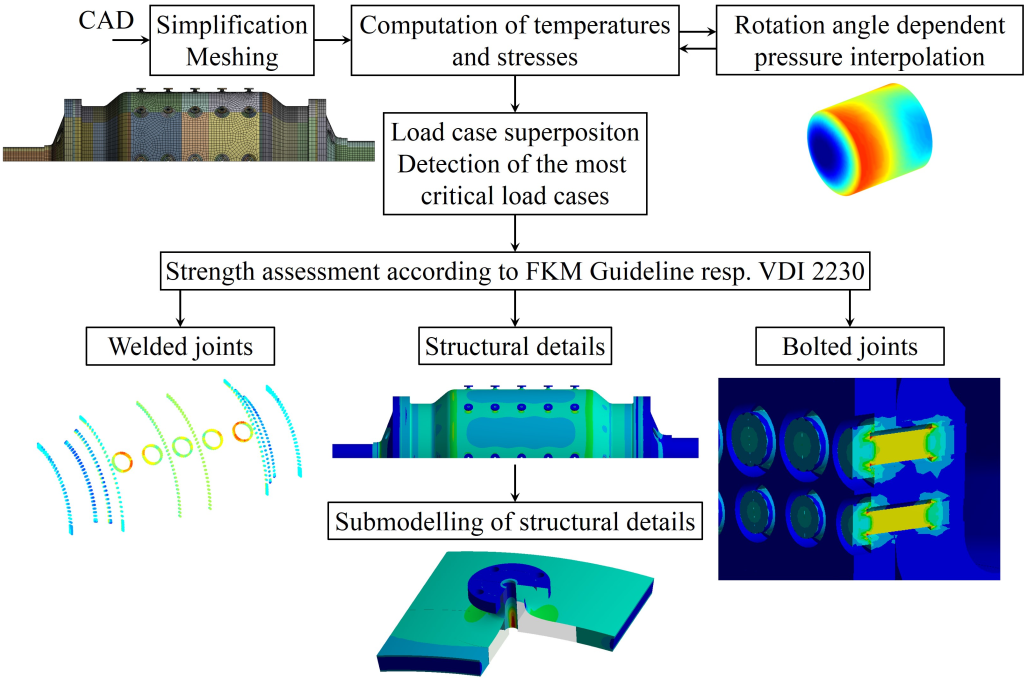

Figure 5: Flowchart of the calculation algorithms for the strength assessment.

the vessel, which is discretized in steps of $5°$, represents the crucial parameter. Regarding the mechanical loads, it is necessary to evaluate a complete stress period. Except for the weight force, all loads appear either in the body-fixed or in the platform-fixed coordinate system. However, since the direction of the weight force coincides with the axis of rotation of the platform, it is identical in the inertial system and in the platform-fixed coordinate system. For this reason, the investigation of one rotation of the vessel about its longitudinal axis is sufficient. Here, in general the load is not symmetric, which requires a full model. The sector-symmetrical design of the pressure vessel allows the reconstruction of a full rotation from a quarter turn. When the load is rotated through $90°$, the stress distribution is equivalent to the case where the container is rotated through $90°$ with an unchanged load direction. The load resulting from the imbalance can be composed of two perpendicular components. That is why one load step is sufficient to determine a complete revolution by using sector symmetry. Due to the complex pressure distribution this procedure cannot be applied for the other mechanical loads.

In order to minimize both the effort involved in the preprocessing and in the postprocessing, a quarter model is created and completed to the full model by $90°$ rotation. The nodes at the interfaces are merged in order to connect the segments. This procedure ensures that each node in the original quarter model has three corresponding nodes in the other segments. Thus, no stress interpolation is needed and the quarter model is sufficient for the strength assessment.

The reduction of the computational effort is demonstrated using the example of the sodium experiment with the precession ratio $\eta = 0.1$ and a certain swivel angle. Instead of computing all combinations of 72 rotation angles, 72 imbalance directions and 16 time steps, the finite element model system only has to be solved for 18 rotation angles, 1 imbalance direction and 16 time steps. Hence, the number of load cases reduces from 82,944 to 35.

The load of the radial imbalance can be adapted to the current angular velocity by scaling and thus to the swivel angle. Besides, this load does not depend on the precession ratio. Furthermore, for the precession ratio $\eta = 0$ a distinction between the platform rotation directions becomes superfluous. Instead of many millions of load cases, the calculation effort is reduced to a few hundred, as illustrated in Figure 7.

In addition, the used linearization has a further advantage. The stiffness matrix always remains constant, while the load vector changes between each load case. As a consequence, the factorization of the system matrix must be performed only once for the quarter model and the full model. Afterwards, the load vector is varied, which reduces the computational costs drastically, especially if sufficient internal memory is available to store the factorized matrix.

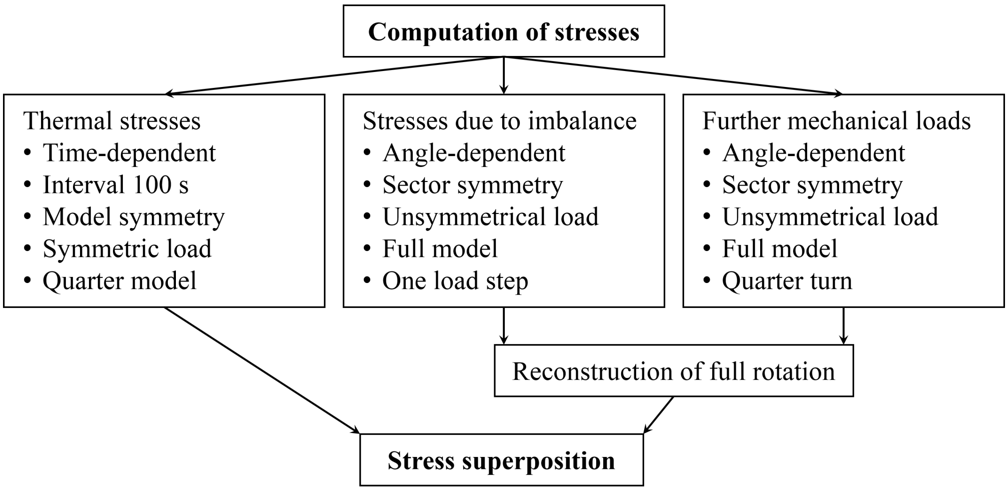

Figure 6: Segmentation of the stress computation to reduce the number of load cases combining the rotational speeds, the gyroscopic effects, the internal pressure and the weight force under further mechanical loads.

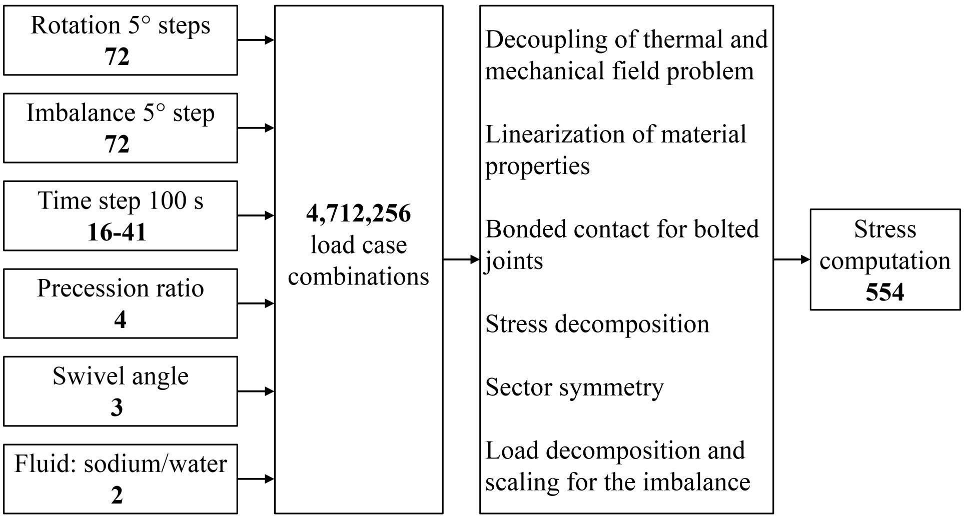

Figure 7: Load case combination and methods to reduce the computational effort. The number of variants is indicated below the variables.

3.2 Load Case Superposition and Strength Assessment

All possible load combinations are reconstructed from the calculated stresses in order to identify the most critical load case for the strength assessment. This is done separately for the static strength and the fatigue strength. According to the FKM Guideline (FKM, 2012) different concepts are applied to assess the non-welded sections and the welded joint. In addition, the bolted joints are examined via VDI 2230 Part 2 (2014).

The evaluation is conducted separately for each node and each bolt respectively with the strength values being always related to the maximum temperature. The fatigue assessment is carried out for an infinite number of load cycles, since the planned operating time of 2000 h with the maximum rotation frequency of 10 Hz corresponds to $7.2 \cdot 10^7$ cycles. This also allows the user-specific distribution of the different swivel angles and precession ratios, because no stress spectrum has to be predefined. The stresses due to the imbalance are constant as the direction does not change during operation. Furthermore, the thermal stresses can be regarded as quasi-static because one temperature cycle consisting of heating and cooling takes several hours, resulting in a frequency, which is many orders of magnitude lower than the rotational frequency. Therefore, the determination of the stress amplitudes is limited to the mechanical loads.

Due to a sufficiently fine mesh, the stresses can be interpreted as local stresses for the non-welded areas. The computational effort is reduced by analyzing only the surface nodes of the quarter model because of the sector symmetry and the fact that a potential crack is expected to start at the surface. For the static strength assessment the maximum von Mises stress is evaluated for all load case superpositions and then the combination with the highest value is determined. Plastic deformations are only taken into account for structural details, where the assessment cannot be provided otherwise. However, the material has high strength reserves by strain hardening that are considered during the strength assessment.

The largest stress amplitude is determined separately for each stress component during a full rotation. In order to obtain an equivalent utilization ratio, the amplitudes are combined according to the von Mises hypothesis. The load case combination with the highest equivalent stress amplitude is considered for the strength assessment. In a second step the influence of the mean stress is taken into account, whereby the fatigue resistance decreases with increasing mean stress. That is why the load case combination with the maximum mean stress is detected including the constant stresses due to the imbalance and the quasi-static thermal stresses, which is used for the calculation of the utilization ratio. Since this is performed separately for every node, supporting effects in the case of high stress gradients are not considered because the determined stresses at adjacent nodes do not necessarily belong to the same load case.

During the strength assessment of welded joints it is necessary to distinguish between butt welds and fillet welds. The stresses at the butt welds can be directly interpreted as local nominal stresses. As the welds are positioned at a sufficient distance from geometrical notches, no high stress gradients occur allowing the use of the fatigue resistance values (FAT classes) for nominal stresses. For the fillet welds structural stresses are considered. However, surface extrapolation (hot-spot method) as recommended by the International Institute of Welding (Hobbacher, 2007) is not feasible for the given geometry. For this reason, the concept of Haibach (Haibach, 1968) is used, according to which the structural stress is determined at a distance of 2 mm from the weld toe. The obtained structural stresses are used only to identify the most critical load cases, which are assessed by effective notch stresses afterwards. Therefore, the weld toes are rounded with a radius of 1 mm (Fricke, 2008). This can only be applied in combination with submodelling techniques because of the very fine mesh and the large number of degrees of freedom. Hence, it is necessary to identify the critical load cases and places for crack initiation in the global model.

The static strength assessment is mainly analogous to the non-welded areas, since only the equivalent stress σ_v

$$\sigma_v = \sqrt{{\sigma_\perp}^2 + {\tau_\|}^2} \tag{2}$$

differs taking into account the stress perpendicular to the weld $\sigma_\perp$ and the shear stress parallel to the weld $\tau_\|$ (FKM, 2012). In the first step of the fatigue strength assessment again the highest stress amplitude is determined, while in the second step the load case combination with the maximum mean stress is detected. According to FKM (2012) the equivalent stress amplitude σ_{av}

$$\sigma_{av} = \frac{1}{2} \cdot \left(|\sigma_{a\perp} + \sigma_{a\|}| + \sqrt{(\sigma_{a\perp} - \sigma_{a\|})^2 + 4 \cdot {\tau_{a\|}}^2} \right) \tag{3}$$

follows, where $\sigma_{a\perp}$ and $\sigma_{a\|}$ describe the amplitudes of the stress components perpendicular and parallel to the weld while $\tau_{a\|}$ stands for the amplitude of the shear stress.

For the bolted joints, the linearized model is used to identify the most critical load cases and the most heavily loaded bolts. Since the components, which should be bolted together, are connected within the non-overlapping clamping area, the contact loads can be used to infer the transmitted load at each bolt. Here, the tensile force as well as the shear force and the bending moment are of particular interest. If materials with different coefficients of thermal expansion are screwed, as in case of the flanges connecting the main assemblies of the vessel, the change of pretension due to heating must be considered. The load case identification is performed separately for the different load components as a weighting with respect to their effect in the nonlinear model is not yet possible. Afterwards, a finite element model of model class III according to VDI 2230 Part 2 (2014) is used for a detailed analyses and the strength assessment. Therefore, the bolts are modeled as equivalent cylindrical volumes. Both the pretension of the bolts and the contact status, including the friction between the clamped components, are taken into account, which inevitably leads to a nonlinear model. However, due to the restriction to a few load cases the computational effort remains manageable. For the static strength assessment the stresses at maximum preload are of interest. In contrast, for the fatigue strength assessment the minimum preload must be applied, considering the tightening factor and the amount of embedding, since the highest stress amplitudes result in this case. The simplified screw model leads to stress singularities under the bolt head and in the thread. That is why the nodal reaction forces are used for the computation of the nominal stresses, which are needed for the strength assessment.

4 Results

The complexity of the vessel does not allow to include all structural details within one finite element model, since the resulting degree of freedom would clearly exceed the computational feasibility. Therefore, a global model is used, first considering only the outer wall of the container and the parts connected to the bearings in detail. The conical ends and the interior walls have a coarse mesh, which does not allow the evaluation of local stresses. However, the model contains the inertial effects and the global deformations of these assemblies. Figure 8 displays the results of the static strength assessment for the outer wall of the vessel. Here, the utilization ratio which is defined as the quotient of the acting stresses and the allowed stress reaches a maximum of approximately 89 %.

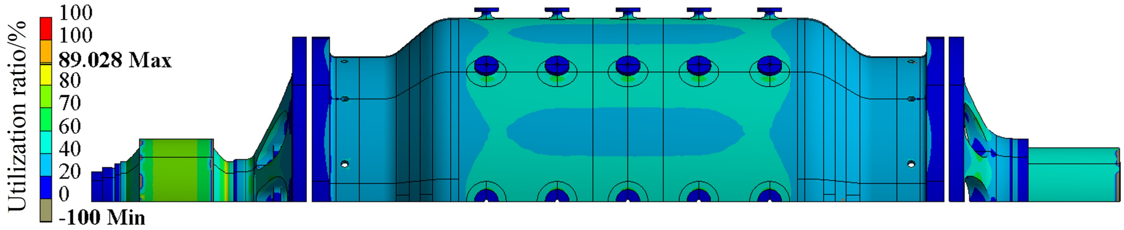

Figure 8: Utilization ratio for the static strength assessment of the vessel.

The result of the fatigue strength assessment of the welded joints is shown in Figure 9. Here, the maximum utilization ratio is 96 %, thus both assessments are fulfilled. The guideline-specific safety factors are already included in these values. The sensor flanges, the cones, the interior assemblies and the bolted joints are examined separately using submodels. Furthermore, the strength assessment of the fillet welds with effective notch stresses requires additional submodels.

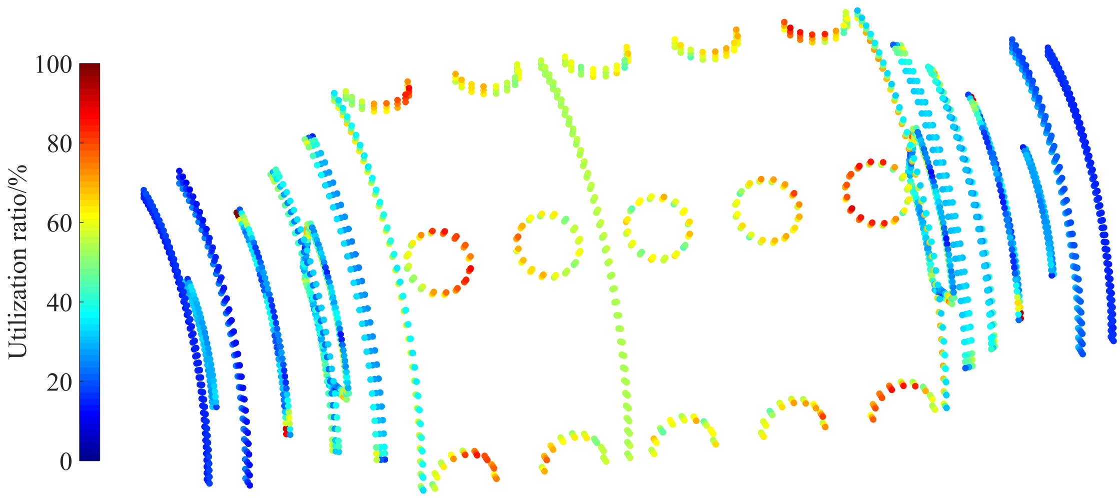

Figure 9: Utilization ratio for the fatigue strength assessment of the welded joints.

5 Summary

A concept was developed for the computational strength assessment of a precession driven dynamo to explore planetary magnetic fields. The various thermal and mechanical loads acting on the pressure vessel lead to several millions of load cases. By decoupling the thermal and mechanical field, linearization, utilization of sector symmetry and dividing the stresses into the thermal stresses, the stresses due to imbalance and the stresses resulting from the other mechanical loads, the computational effort is drastically reduced by several orders of magnitude. Stress superposition allows to identify the most critical load cases and load case combinations respectively needed for the strength assessment. Therefore, it must be distinguished between the non-welded structure and the welded joints. In both cases the FKM Guideline is used, while the bolted joints are proved according to VDI 2230.

References

FKM Forschungskuratorium Maschinenbau: *FKM-Richtlinie Rechnerischer Festigkeitsnachweis für Maschinenbauteile aus Stahl, Eisenguss- und Aluminiumwerkstoffen*, vol. 6. VDMA-Verlag GmbH, Frankfurt (2012).

Fricke, W.: Guideline for the Fatigue Assessment by Notch Stress Analysis for Welded Structures. In: *Annual Assembly of International Institute of Welding*, IIW-Doc. XIII-2240r2-08/XV-1289r2-08 (2008).

Giesecke, A.; Albrecht, T.; Gerbeth, G.; Gundrum, T.; Stefani, F.: Numerical simulations for the DRESDYN precession dynamo. *Magnetohydrodynamics*, 51, (2014), 293–302.

Haibach, E.: Die Schwingfestigkeit von Schweißverbindungen aus der Sicht einer örtlichen Beanpsruchungsmessung. Tech. rep., Fraunhofer-Inst. für Betriebsfestigkeit, Darmstadt (1968).

Hobbacher, A.: Recommendations for the Fatigue Design of Welded Joints and Components. Tech. rep., International Institute of Welding, Paris (2007).

Stefani, F.; Albrecht, T.; Gerbeth, G.; Giesecke, A.; Gundrum, T.; Herault, J.; Nore, C.; Steglich, C.: Towards a precession driven dynamo experiment. *Magnetohydrodynamics*, 51, (2014), 275–284.

Stefani, F.; Eckert, S.; Gerbeth, G.; Giesecke, A.; Gundrum, T.; Steglich, C.; Weier, T.; Wustmann, B.: DRESDYN - A new facility for MHD experiments with liquid sodium. *Magnetohydrodynamics*, 2012, (2012), 103–113.

Stefani, F.; Gailitis, A.; Gerbeth, G.: Magnetohydrodynamic experiments on cosmic magnetic fields. *ZAMM - Zeitschrift für Angewandte Mathematik und Mechanik*, 88(12), (2008), 930–954.

VDI-Fachbereich Produktentwicklung und Mechatronik: *VDI 2230 Part 1 Systematic calculation of highly stressed bolted joints - Joints with one cylindrical bolt*. VDI-Gesellschaft Produkt- und Prozessgestaltung (2014).

VDI-Fachbereich Produktentwicklung und Mechatronik: *VDI 2230 Part 2 Systematic calculation of highly stressed bolted joints - Multi bolted joints*. VDI-Gesellschaft Produkt- und Prozessgestaltung (2014).

Address: TU Dresden, Chair of Dynamics and Mechanism Design, Marschnerstr. 30, 01307 Dresden, Germany
email: stephan.rother@tu-dresden.de